

# Evaluation of a simple parameterization of the Evaporative Stress Index using FLUXNET data and a planetary boundary layer model

Nicole Keeney<sup>1</sup> and Dennis Baldocchi<sup>2</sup>

<sup>1</sup>*Department of Earth and Planetary Science, University of California, Berkeley, California, USA*

<sup>2</sup>*Department of Environmental Science, Policy, and Management, University of California, Berkeley, California, USA*

---

The Evaporative Stress Index (ESI) is a drought index that describes temporal anomalies in evapotranspiration, providing an important measure of ecosystem water stress and soil moisture deficits. We evaluate a simple parameterization of ESI introduced by Fisher et al. (2008) as a soil moisture constraint that is reliant only on relative humidity, vapor pressure deficit, and a power law parameter, greatly reducing the number of input parameters required and allowing for calculation of soil moisture deficits using atmospheric variables that can be easily measured from space. Calculation of ESI is typically dependent on complex parameterizations of evapotranspiration and knowledge of the surface energy budget, with limited utility if all input variables are not known or if measurement error is large. Evaluations of our proposed ESI parameterization using both a planetary boundary layer model and eddy covariance tower data from FLUXNET 2015 indicate that the model is a good approximation of ESI, particularly when the power law parameter is calculated by ecotype. Our analysis suggests that biosphere-atmosphere interactions, which directly impact vapor pressure deficit and relative humidity, can provide a simple but effective measure of soil moisture deficits.

---

## 1. Introduction

Understanding the spatial and temporal distribution of ecosystem water use is a key component of identifying regions currently undergoing or at risk of drought. Given that anthropogenic climate change is shifting many arid regions toward warmer and drier climates, along with increasing the frequency and intensity of extreme precipitation events, it is pertinent to

have accurate and easily accessible information on ecosystem water stress (Easterling et al., 2000; Stocker et al., 2013).

Assessing drought conditions requires routine measurement of soil moisture deficits on large spatial scales. While remote sensing data can provide useful estimates of soil moisture, satellites can only accurately detect water in the first few centimeters of soil (Wang et al., 2009). Considering that many plants have deep roots, with some plants capable of tapping into groundwater reserves, the moisture content in the top layer of soil can only provide a limited view of ecosystem water use (Fan et al., 2017). Remote sensing-derived models of evapotranspiration, such as the Priestley-Taylor Jet Propulsion Laboratory model, rely on partitioning and parameterizing contributing surface processes (Talsma et al., 2018). Furthermore, remote sensing-derived estimates of the components used to calculate evapotranspiration exhibit large deviations between models as well as significant errors from field estimates (Talsma et al., 2018). Given the challenges and limitations of measuring the soil moisture budget from space, it's necessary to continue evaluating and improving upon existing models.

The evaporative stress index (ESI) is an evapotranspiration-based drought index that describes soil moisture deficits (Anderson, 2011). ESI is defined as the ratio of actual evapotranspiration to potential evapotranspiration and is typically computed using remote sensing-derived estimates of evapotranspiration. In this study, however, we evaluate a model for ESI introduced by Fisher et al. (2008) as a soil moisture constraint ( $f_{SM}$ ) that is based on the principle that ecosystem water stress—and therefore soil moisture deficits—can be determined from the water vapor content of the surrounding atmosphere. This assumption is based on previous research indicating that stomatal closure exhibits considerable control over transpiration when soil water supply is limiting, while transpiration under well-watered conditions is largely driven by available energy (Jarvis and McNaughton, 1986). This concept describes the feedback of the planetary boundary layer to surface fluxes, such that an increase in surface transpiration causes humidification and growth of the planetary boundary layer (Jacobs and De Bruin, 1992). Thus, we expect atmospheric water vapor content to reflect soil moisture conditions, considering that transpiration drives transport of water up the soil-plant-atmosphere continuum. Using relative humidity (RH) and vapor pressure deficit (VPD) as a measure of atmospheric water

vapor, Fisher et al. (2008) defines a relationship between soil and atmospheric moisture given by:

$$f_{SM} = RH^{VPD/\beta}$$

where the exponential relationship between RH and VPD describes the nonlinearity of  $f_{SM}$  in response to anomalously high and low VPD values. The power law parameter  $\beta$  defines sensitivity of the system to VPD and is computed in our analysis.

In this study, we test the mechanism and utility of the  $f_{SM}$  model for the evaporative stress index using a planetary boundary layer model and eddy covariance tower data representing a range of different ecotypes. We demonstrate the strength of the model in assessing water stress experienced by dryland ecosystems, which frequently experience drought. Our results indicate that plant-atmosphere interactions can act as a sensor for soil moisture deficits over large time scales.

## 2. Materials and Methods

### 2.1. Model evaluation with FLUXNET 2015 data

We evaluate the  $f_{SM}$  model with data from FLUXNET, a global network of eddy covariance towers that provide in-situ measurements of scalar and energy fluxes (Pastorello et al., 2020). We include in our analysis all towers from the FLUXNET 2015 dataset that provide measurements for vapor pressure deficit, relative humidity, air temperature, air pressure, net radiation, soil heat flux, and latent heat flux. This subset includes a total of 146 towers representing 10 different ecotypes, with over a decade of data collection for many towers. An advantage to using the FLUXNET 2015 dataset is that all measurements have been quality checked and gap-filled using the same methods, assuring that data processing is uniform between different sites. We compute monthly averages for our analysis, reducing noise from daily measurements and allowing for the assumption that the system is at equilibrium.

Monthly averaged data is used to compute ESI as originally defined as the ratio of actual to potential evapotranspiration at every data point for each tower. Actual evapotranspiration is given by the latent heat flux, and we calculate potential evapotranspiration using the Priestley Taylor model (Priestley and Taylor, 1972):

$$ET = \alpha \frac{s}{s + \gamma} (R_{\text{net}} - G)$$

where net radiation ( $R_{\text{net}}$ ) and soil heat flux ( $G$ ) are provided as direct measurements from the eddy covariance towers. We use a Priestley Taylor constant ( $\alpha$ ) of 1.26, consistent with previous research for a well-watered canopy model (Priestley and Taylor, 1972; De Bruin, 1983). The slope of the saturation vapor pressure-temperature curve ( $s$ ) is calculated by taking the derivative of saturation vapor pressure in respect to air temperature at each data point. The psychrometric constant ( $\gamma$ ), which describes the relationship between air temperature and the partial pressure of water in the air, is similarly computed at each data point.

Using the relationship between relative humidity and the evaporative stress index computed from FLUXNET data, we derive a value for the power law parameter  $\beta$  required for evaluation of the  $f_{SM}$  model. The Broyden-Fletcher-Goldfarb-Shanno optimization algorithm is applied to solve for a best fit  $\beta$  value in python. We report an overall  $\beta$  value along with a value for individual ecotypes in the Results and Discussion section. The ecotype assignment describes the vegetation type based on the International Biosphere-Geosphere Programme definition and is provided by the PI of each tower. Ecotypes included in the 146 tower sites are: Croplands, Closed Shrublands, Deciduous Broadleaf Forests, Evergreen Broadleaf Forests, Evergreen Needleleaf Forests, Grasslands, Mixed Forests, Open Shrublands, Savannas, Permanent Wetlands, and Woody Savannas. Using the derived  $\beta$  value,  $f_{SM}$  is computed using vapor pressure deficit and relative humidity values at each data point in the FLUXNET 2015 dataset.

## 2.2. *Energy balance - planetary boundary layer model*

The theoretical validity of the  $f_{SM}$  model relies on the assumption that soil moisture deficits are reflected in the water content of the planetary boundary layer, such that plant-atmosphere interactions can be used as the ultimate sensor of ecosystem water stress. To test the mechanism and utility of this concept, we use a coupled surface energy balance - planetary boundary layer growth model (Baldocchi and Ma, 2013; McNaughton and Spriggs, 1986; Paw and Gao, 1988). A detailed description of the model used is given in Baldocchi and Ma (2013) and thus is omitted from this paper.  $f_{SM}$  is computed with simulated relative humidity and vapor pressure values at each time step and a best-fit  $\beta$  value derived for the model. We initialize the model with an

albedo of 0.2 (Hollinger et al. 2010) and incoming solar radiation of  $1000 \text{ W/m}^2$ , representing meteorological and surface conditions typical of a grassland ecosystem in the summer. Model simulations and data analysis are performed in MATLAB.

### 3. Results and Discussion

We subdivided the 146 FLUXNET tower sites by ecotype to evaluate the performance of the  $f_{SM}$  model in different climatic and vegetation conditions. A best fit  $\beta$  was derived for each ecotype and used to compute  $f_{SM}$  at each relative humidity value. While wet, well-watered ecotypes, including wetlands, croplands, and evergreen forests, show poor fit to the  $f_{SM}$  model, dryland ecosystems show considerable overlap between modelled and measured ESI. Because the evaporative stress index serves to identify regions of water stress, strong performance of the  $f_{SM}$  model is not expected in ecosystems that do not frequently experience significant water stress. Results for savanna, woody savanna, and grassland ecotypes are presented in Figure 1, illustrating the relationship between relative humidity and the evaporative stress index that provides the basis for the  $f_{SM}$  model. Derived  $\beta$  values are 1.28, 0.95, and 0.78 respectively, and we find a predominantly linear function for  $f_{SM}$ .

Figure 1 also shows combined data from savannas, woody savannas, and grasslands ecotypes, representing 2106 total monthly averaged values from 42 tower sites from which a combined  $\beta$  value of 0.91 is derived. The  $f_{SM}$  model appears to capture the overall trend of ESI values for grasslands and savannas, but significant variability in measured ESI results in a RMSE of 0.23 and a low correlation coefficient ( $r^2$ ) of 0.22 when comparing measured to modelled values, reflecting the limitations of a simplified model (Figure 2). Evaluation of the residuals (measured ESI  $- f_{SM}$ ) by relative humidity indicate that the model underestimates ESI at low relative humidity and overestimates ESI at high relative humidity, suggesting that other environmental factors must be incorporated in the parameterization in order to improve the overall precision of the model (Figure 3). However, given sufficiently large temporal time scales and long data records, strong overlap between the  $f_{SM}$  model and measured ESI demonstrate that  $f_{SM}$  can provide a good indication of ecosystem water stress over time for dryland ecosystems.

While variability in natural ecosystems limits the precision of the  $f_{SM}$  model for field measurements,  $f_{SM}$  exhibits strong performance with the energy balance – planetary boundary

layer (PBL) model simulations (Figures 4-5). ESI is computed using simulated fluxes at each time step as the ratio of latent heat flux to potential evapotranspiration, where potential evapotranspiration is derived from the Priestley Taylor model. The growth of the planetary boundary layer and associated surface energy and scalar fluxes are simulated hourly for 5 boundary layer resistance values and 9 stomatal resistance values over a 45-day period, representing 1080 total simulations. The data has been averaged daily to reduce noise from hourly variability. ESI vs.  $f_{SM}$  has an  $r^2$  of 0.95 as illustrated in Figure 5, indicating strong fit of  $f_{SM}$  to ESI.

Savannas and grasslands are characterized by moisture limitations, periodic drought, and an arid climate (Faber-Langendoen et al., 2016). Seasonal dependence on rainfall and intermittent occurrence of drought results in extensive variability in soil moisture across seasonal, annual, and decadal timescales (James et al., 2003; Quesada et al. 2006). Considering sufficiently long time periods, our results demonstrate that relative humidity and the evaporative stress index for savannas and grasslands encompass the entire range of possible values, from extremely dry periods characterized by soil moisture limitations to well-watered periods in which actual evapotranspiration approaches potential evapotranspiration. Results from the energy balance – planetary boundary layer model and analysis of FLUXNET tower data illustrate a predominately linear relationship between relative humidity and the ESI for dryland ecosystems. For well-watered ecotypes, however, tower data shows clumping and scattering of relative humidity and ESI at high values, with no strong trend in the data. For ecotypes that do not exhibit a clear relationship between relative humidity and ESI, the  $f_{SM}$  model fails. We therefore emphasize that  $f_{SM}$  can only appropriately describe soil moisture conditions for dryland ecosystems.

#### 4. Conclusion

We evaluate  $f_{SM} = RH^{VPD/\beta}$  as a parameterization for the evaporative stress index using both field measurements from FLUXNET 2015 and simulated energy fluxes from a planetary boundary layer model. Savanna and grassland ecosystems show good fit to the  $f_{SM}$  model when using data that has been averaged over sufficiently long temporal scales. Strong performance of  $f_{SM}$  when validated with planetary boundary layer model simulations and substantially weaker performance of  $f_{SM}$  using field measurements illustrates the complexities of assessing soil

moisture deficits in a natural environment. Our analysis of  $f_{SM}$  demonstrates how the gradual adjustment and feedbacks between the planetary boundary layer, relative humidity, and surface fluxes can provide a simple but effective mechanism for measuring soil moisture deficits. Further evaluation of  $f_{SM}$  using remote-sensing derived measurements of the evaporative stress index provided by the ECOSTRESS mission would allow for a better understanding of the mechanism and utility of the model.

## 5. References

- Anderson, M., Hain, C., Wardlow, B., Pimstein, A., Mecikalski, J., & Kustas, W. (2011). Evaluation of drought indices based on thermal remote sensing of evapotranspiration over the continental united states. *Journal of Climate*, 24, 2025-2044. <https://doi.org/10.1175/2010JCLI3812.1>
- Baldocchi, Dennis & Ma, Si Yan. (2013). How will land use affect air temperature in the surface boundary layer? Lessons learned from a comparative study on the energy balance of an oak savanna and annual grassland in California, USA. *Tellus B*. 65.10.3402/tellusb.v65i0.19994.
- De Bruin, H. A. R., & Holtslag, A. A. M. (1982). A simple parameterization of the surface fluxes of sensible and latent heat during daytime compared with the Penman-Monteith concept. *Journal of Applied Meteorology and Climatology*, 21(11), 1610-1621. [https://doi.org/10.1175/15200450\(1982\)021<1610:ASPOTS>2.0.CO;2](https://doi.org/10.1175/15200450(1982)021<1610:ASPOTS>2.0.CO;2)
- Easterling, D. R., Meehl, G. A., Parmesan, C., Changnon, S. A., Karl, T. R., & Mearns, L. O. (2000). Climate extremes: Observations, modeling, and impacts. *Science*, 289(5487), 2068-2074. <https://doi.org/10.1126/science.289.5487.2068>
- Fan, Y., Miguez-Macho, G., Jobbágy, E. G., Jackson, R. B., & Otero-Casal, C. (2017). Hydrologic regulation of plant rooting depth. *Proc Natl Acad Sci USA*, 114(40), 10572. <https://doi.org/10.1073/pnas.1712381114>
- Fisher, J. B., Tu, K. P., & Baldocchi, D. D. (2008). Global estimates of the land-atmosphere water flux based on monthly AVHRR and ISLSCP-II data, validated at 16 FLUXNET sites. *Remote Sensing of Environment*, 112(3), 901-919. <https://doi.org/10.1016/j.rse.2007.06.025>
- Hollinger, D.Y., Ollinger, S.V., Richardson, A.D., Meyers, T.P., Dails, D.B., Martin, M.E., Scott, N.A., Arkebauer, T.J., Clark, K.L. (2010). Albedo estimates for land surface models and support for a new paradigm based on foliage nitrogen concentration. *Global Change Biology*. 16(2): 696-710.
- IPCC, 2013: Climate Change 2013: The Physical Science Basis. Contribution of Working Group I to the Fifth Assessment Report of the Intergovernmental Panel on Climate Change [Stocker, T.F., D. Qin, G.-K. Plattner, M. Tignor, S.K. Allen, J. Boschung, A. Nauels, Y. Xia, V. Bex and P.M. Midgley (eds.)]. *Cambridge University Press*, Cambridge, United Kingdom and New York, NY, USA, 1535 pp, doi:10.1017/CBO9781107415324.
- Jacobs, C. M. J., & de Bruin, H. A. R. (1992). The sensitivity of regional transpiration to land surface characteristics: Significance of feedback. *Journal of Climate*, 5(7), 683-698. <http://www.jstor.org/stable/26197103>
- James, S. E., Pärtel, M., Wilson, S. D., & Peltzer, D. A. (2003). Temporal heterogeneity of soil moisture

- in grassland and forest. *Journal of Ecology*, 91(2), 234-239.  
<https://doi.org/10.1046/j.1365-2745.2003.00758>.
- Jarvis, P., & McNaughton, K. (1986). Stomatal Control of Transpiration: Scaling Up from Leaf to Region. *Advances in Ecological Research*, 15, 1-49.
- McNaughton, K. G., & Spriggs, T. W. (1986). A mixed-layer model for regional evaporation. *Boundary Layer Meteorology*, 34(3), 243-262. <https://doi.org/10.1007/BF00122381>
- Pastorello, G., Trotta, C., Canfora, E., Chu, H., Christianson, D., Cheah, Y., Poindexter, C., Chen, J., Elbashandy, A., Humphrey, M., Isaac, P., Polidori, D., Ribeca, A., van Ingen, C., Zhang, L., Amiro, B., Ammann, C., Arain, M. A., Ardö, J., . . . Papale, D. (2020). The FLUXNET2015 dataset and the ONEFlux processing pipeline for eddy covariance data. *Scientific Data*, 7(1), 225. <https://doi.org/10.1038/s41597-020-0534-3>
- Paw U, K. T., & Gao, W. (1988). Applications of solutions to non-linear energy budget equations. *Agricultural and Forest Meteorology*, 43(2), 121-145. [https://doi.org/10.1016/0168-1923\(88\)90087-1](https://doi.org/10.1016/0168-1923(88)90087-1)
- Priestley, C, & Taylor, R. (1972). On the assessment of surface heat flux and evaporation using large scale parameters. *Monthly Weather Review*, 100(2), 81-92. [https://doi.org/10.1175/1520-0493\(1972\)100<0081:OTAOSH>2.3.CO;2](https://doi.org/10.1175/1520-0493(1972)100<0081:OTAOSH>2.3.CO;2)
- Quesada, C., Hodnett, M., Breyer, L., Santos, A., Andrade, S., Miranda, H., Miranda, A., & Lloyd, J. (2008). Seasonal variations in soil water in two woodland savannas of central brazil with different fire history. *Tree Physiology*, 28, 405-15. <https://doi.org/10.1093/treephys/28.3.405>
- Talsma, C. J., Good, S. P., Jimenez, C., Martens, B., Fisher, J. B., Miralles, D. G., McCabe, M. F., & Purdy, A. J. (2018). Partitioning of evapotranspiration in remote sensing-based models. *Agricultural and Forest Meteorology*, 260-261, 131-143. <https://doi.org/10.1016/j.agrformet.2018.05.010>
- Wang, L., & Qu, J. (2009). Satellite remote sensing applications for surface soil moisture monitoring: A review. *Frontiers of Earth Science in China*, 3, 237-247. <https://doi.org/10.1007/s11707-009-0023-7>



## 6. Figures

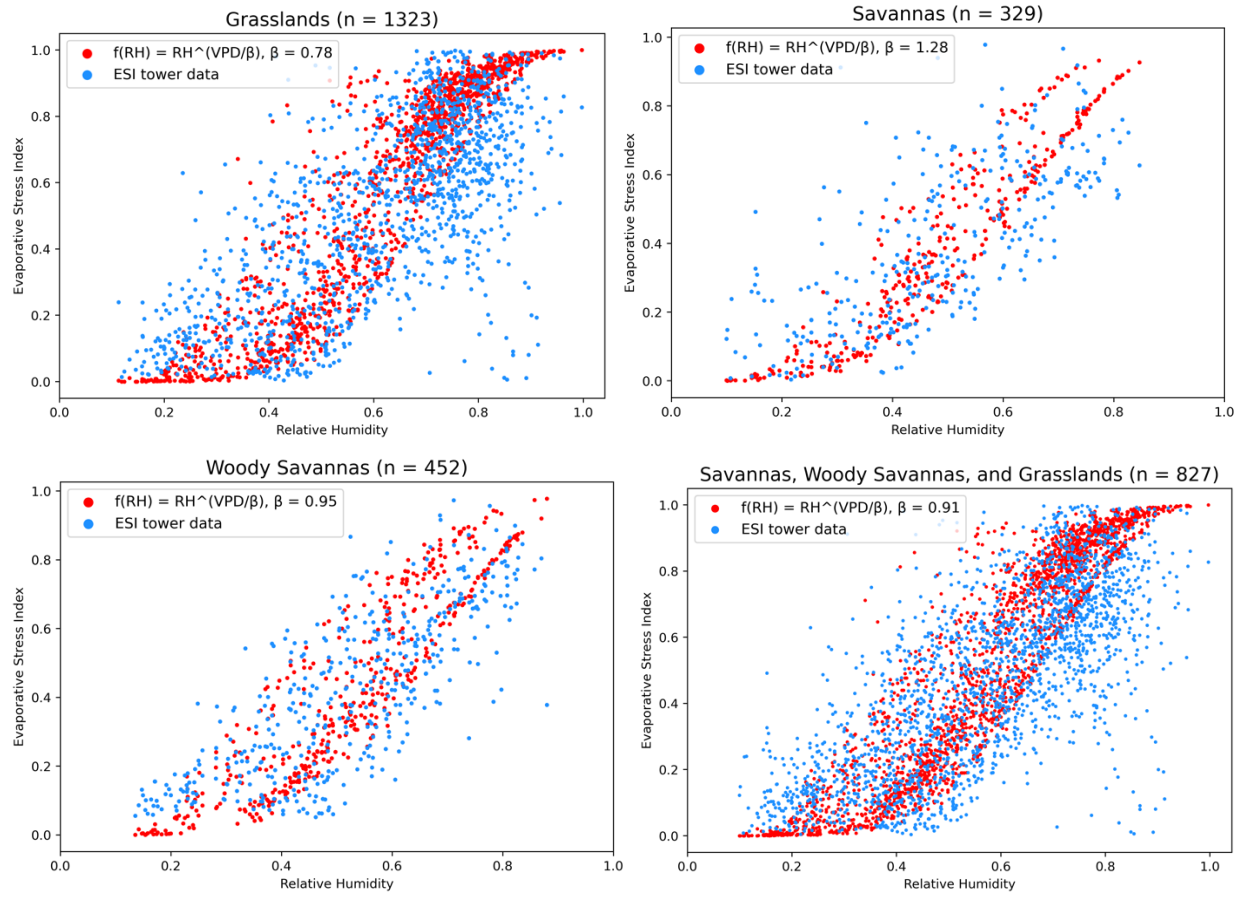


Fig. 1. Evaporative stress index vs. relative humidity for three different ecotypes and their combined effect (bottom right). Red circles are  $f_{SM}$  and blue circles are ESI derived from eddy covariance tower data.

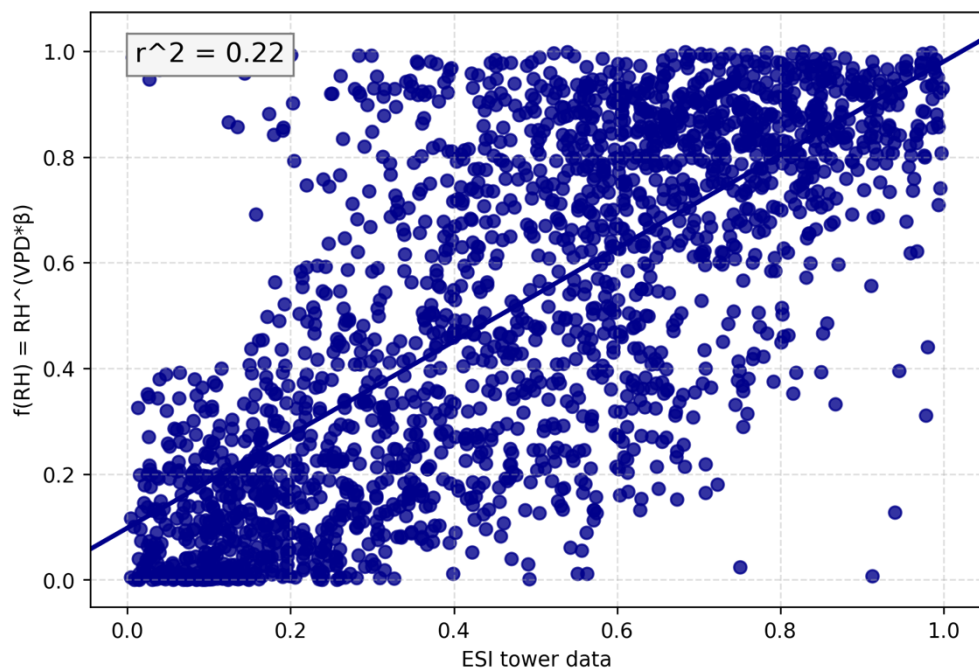


Fig. 2.  $f_{SM}$  vs. ESI derived from eddy covariance tower data

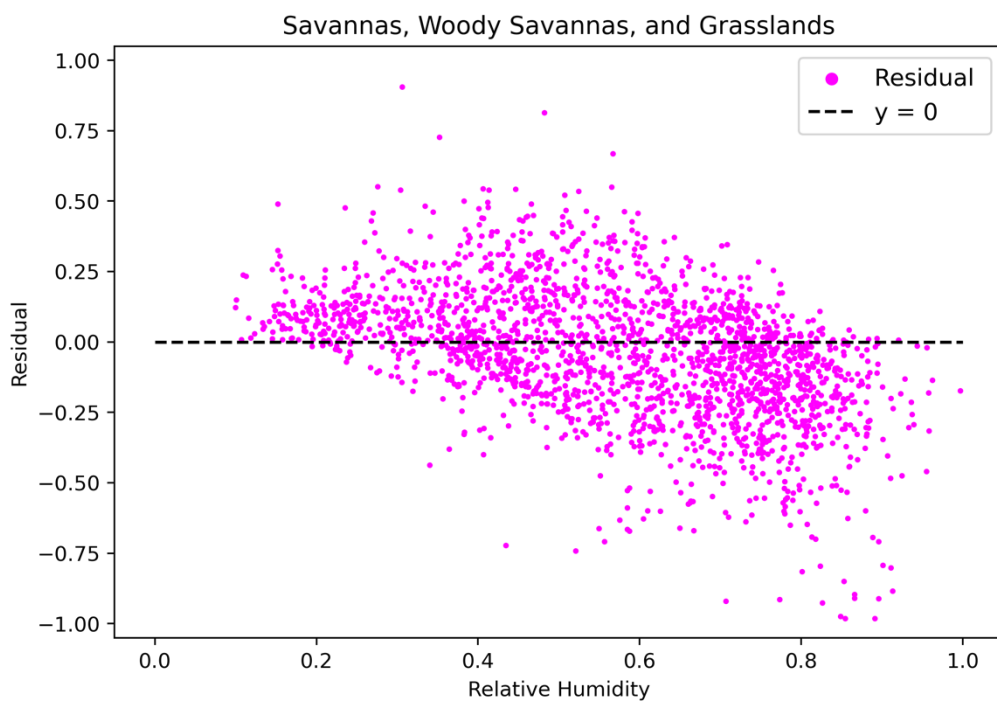


Fig. 3. Residuals (measured ESI -  $f_{SM}$ ) for the combined Savannas, Woody Savanna, and Grassland ecotypes

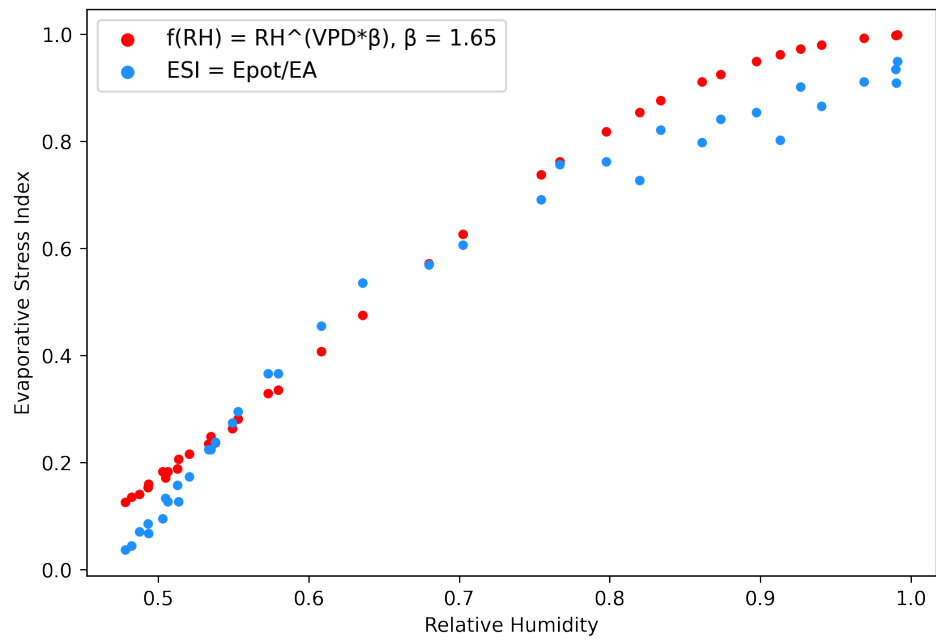


Fig. 4. Evaporative stress index vs. relative humidity derived from the ET-PBL model simulations. Red circles are  $f_{SM}$  and blue circles are  $ESI = E_{Potential}/E_{Actual}$ .

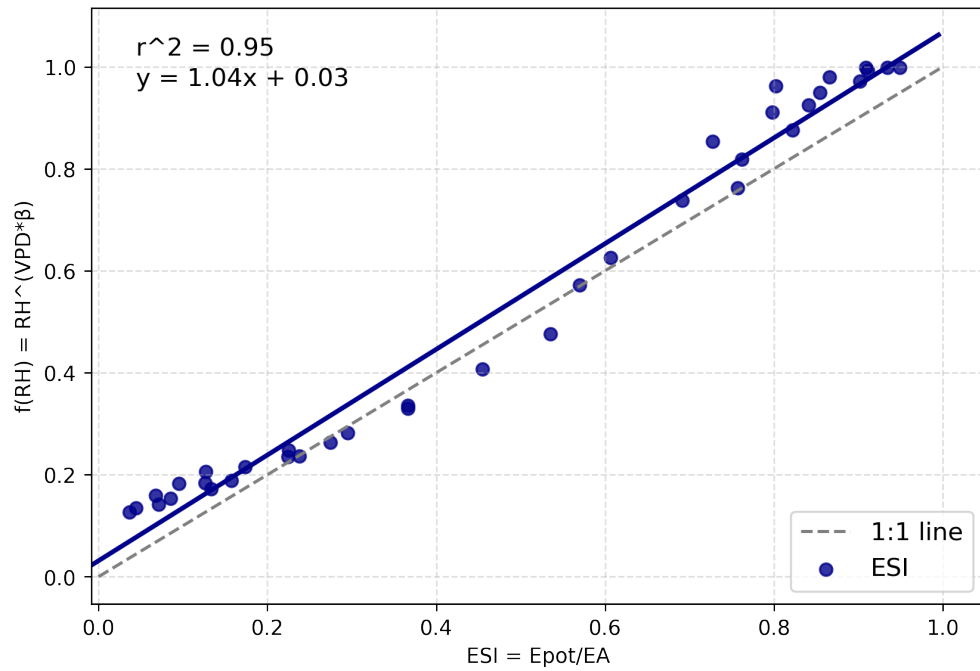


Fig. 5.  $f_{SM}$  vs.  $ESI = E_{Potential}/E_{Actual}$  from ET-PBL model simulations.